Study on Groove Shape Optimization for Micromixers

Mranal Jain, Abhijit Rao and K. Nandakumar*
Cain Department of Chemical Engineering, Louisiana State University
* Corresponding author: 110 Chem. Eng. Bldg., LSU, Baton Rouge, LA 70803, nandakumar@lsu.edu

Abstract: The conventional T-mixer design requires longer channel lengths and times to achieve complete mixing owing to its dependence on transverse diffusion. The performance of a homogeneous T-mixer can be enhanced significantly by the stimulation of secondary/ transverse flows in the microchannel. The groove based micromixers generate helical flows within the microchannel to augment the mixing performance. These micromixers are extensively studied with respect to planar geometric parameters such as groove width, groove spacing, channel height etc. The effect of groove shape is not systematically studied with respect to mixing performance. Previous studies have focused on two or three different groove shapes, typically involving slanted grooves, asymmetric herringbone grooves and their variations. In this computational study, we analyze the effect of groove shape on micromixing performance and search for the optimal groove shape. The groove shape is parametrically represented by Bézier curves which could take any shape within a constrained envelope. The control points of Bézier curve are chosen as optimization parameters to identify the optimal groove shape which maximizes the mixing for given operating conditions. The resulting optimal design generates the most favorable flow structure & concentration distribution for enhanced mass transfer. Various parametric studies are carried out to compare the optimal groove structure with other groove types (slanted groove, herringbone etc.) micromixers.

Keywords: Micromixer, Optimization.

1. Introduction

Micromixers are a vital component of bio-microfluidics devices utilized for complex enzyme reactions biochemical analysis etc. The performance of micro-mixers directly relates to the analysis time as well as device portability. The micromixers can be categorized into active and passive mixers [1] depending upon their mixing strategy. The simplest passive micro-mixer is a T-mixer or Y-mixer, where two confluent streams mix primarily due to transverse diffusion. The mixing performance in passive mixers can be enhanced using geometric modifications as reported for obstacle based micro-mixing heterogeneous charged walls/ bottom, grooves patterning on channel base etc. [1-4]. In general, such geometric/ surface changes generate non-axial flow resulting in improved mixing. On the other hand, active mixers utilize external energy—via pressure, electro-kinetic disturbance etc.—to induce transverse flows [1-2].

In this work, we study the groove based micromixers and investigate the effect of groove shape on the micromixing performance. Stroock et al. [3] proposed the chaotic micromixer design with grooves at the channel bottom wall for pressure driven flows. They studied staggered herringbone groove & slanted groove shapes and found the groove based micromixing ideal for low Reynolds number flows. Johnson et al. [4] investigated the effect of slanted grooves on mixing performance for electrokinetic micromixer. Various studies are reported for groove based micromixers [5-6]; however none of the studies have evaluated the effect of groove shape on mixing performance. This study focuses on the impact of groove shape on the transverse flows and mixing performance. For electrokinetic micromixers, the improved mixing performance has been achieved with shape optimization techniques [7]. The details of mathematical model and optimization are presented in the next section.

2. Mathematical Model

A three-dimensional microchannel domain with grooves at the bottom surface is considered as the computational domain. The schematic for the geometry is shown in Figure 1 with symmetric herringbone type of groove. A total of 60 grooves are axially distributed in form of 10 groove cycles containing 6 grooves per cycle (Figure 1a). The cross-sectional (y-z plane) view for the geometry is shown in Figure 1b and the

geometric parameters along are outlined in Table 1 (Appendix 1).

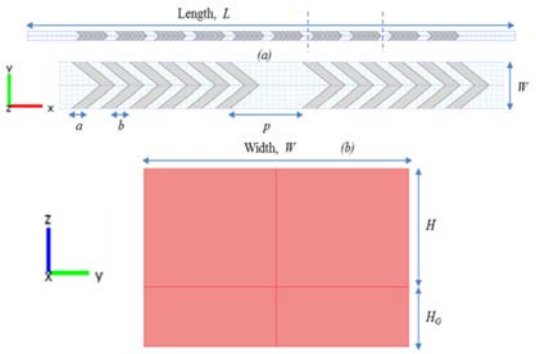

Figure 1. The channel geometry is shown (a) the x-y plane view of the geometry with axial arrangement of groove structure and; (b) the y-z plane (cross-sectional) view

The solution is treated as an incompressible Newtonian fluid with constant viscosity, and density. To describe the mathematical model, we introduce the following reference quantities and dimensionless variables:

$$L_{\text{ref}} = W, \quad c_{\text{ref}} = c_{0,} \quad u_{\text{ref}} = u_{av} = \frac{Q}{WH}, \quad p_{ref} = \frac{\mu u_{av}}{W}, \text{and}$$

$$\bar{x}=\frac{x}{L_{\text{ref}}}, \quad \bar{y}=\frac{y}{L_{\text{ref}}}, \quad \bar{z}=\frac{z}{L_{\text{ref}}}, \quad \bar{u}=\frac{u}{u_{\text{ref}}}, \quad \bar{v}=\frac{v}{u_{\text{ref}}}, \quad \bar{w}=\frac{w}{u_{\text{ref}}}, \quad \bar{p}=\frac{p}{p_{\text{ref}}}$$

Here W is the channel width, H is the channel height and Q is the axial volumetric flow rate. The species concentration and fluid velocities in x, y & z direction are denoted by c, u, v & w respectively.

The flow field in the computational domain is governed by the continuity and Navier-Stokes equations. These equations, in their dimensionless forms, are:

$$Re(\bar{u}\cdot\bar{\nabla}\bar{u}) = -\bar{\nabla}\bar{p} + \bar{\nabla}^2\bar{u} \qquad 1(a)$$

$$\bar{\nabla}\cdot\bar{u} = 0 \qquad 1(b)$$

In the above equations, Re is the Reynolds number (ratio of inertial to viscous forces) and is given by the following equation:

$$Re = \frac{\rho\, u_{av}\, L_{ref}}{\mu} \qquad (2)$$

The steady transport of species is governed by the convection-diffusion equation. Using the predefined reference quantities and scales, the convection- diffusion can be written in the non-dimensional form as follows:

$$Pe(\bar{u}\cdot\bar{\nabla}\bar{c}) = \bar{\nabla}^2\bar{c} \qquad (3)$$

In the above equation, the Peclet number is defined as:

$$Pe = \frac{u_{ref} L_{ref}}{D} = \frac{Q}{HD} \qquad (4)$$

At the channel walls, the zero flux condition is imposed for the species, while the convective-flux-only boundary condition is applied at the channel outlet. For species transport, a constant concentration condition is imposed at the channel inlets (i.e. scaled concentrations of 0 and 1 at inlet plane 1 $\{\bar{x}=0,-0.5<\bar{y}<0,0<\bar{z}<0.2\}$ and inlet plane 2 $\{\bar{x}=0,\bar{y}<0.5,0<\bar{z}<0.2\}$ respectively). The discontinuity in the inlet concentration is treated using a smoothed Heaviside function (in-built in Comsol Multiphysics).

The mixing performance is typically evaluated by quantifying the deviation from the perfectly mixed state [7] as shown below:

$$\eta = \left[1 - \frac{\sqrt{\frac{1}{N}\sum_{1}^{N}\left(\bar{c} - \bar{c}^{*}\right)^2}}{\sqrt{\frac{1}{N}\sum_{1}^{N}\left(\bar{c}^{0} - \bar{c}^{*}\right)^2}}\right] \qquad (5)$$

In the above equation, N is the number of points in the cross-section used for estimation of the mixing index. The variable $\bar{c}$ represents the scaled concentration value at that point, while $\bar{c}^{0}$ and $\bar{c}^{*}$ are the scaled concentration at each point if the solutions are unmixed and the concentration with perfect mixing (i.e. 0.5), respectively. Based on the mixing index definition (equation 5), the theoretical limits for η is between zero and one.

3. Optimization Approach

The effect of groove shape on the micromixing performance is investigated through parametric representation of groove edge by the Bézier curves. In this preliminary study, single groove shape is being parameterized and subsequently same shape is applied to all the grooves in the channel. The groove edge along the channel width (W) is represented by two cubic Bézier curves with positional continuity.

The Bézier curves are parametric curves defined using the Bernstein polynomials and control points (vertices of a control polygon). A Bézier curve of n^{th} degree with n+1 control points are represented by the following equation:

$$P(t) = \sum_{i=0}^{n} B_i J_{n,i}(t) \qquad 0 \le t \le 1 \qquad (6)$$

In the above equation, B_i represents the control points of the Bézier curve and $J_{n,i}(t)$ are the Bernstein basis polynomials described as follows:

$$J_{n,i}(t) = \frac{n!}{i!(n-i)!} t^i (1-t)^{n-i} \qquad (7)$$

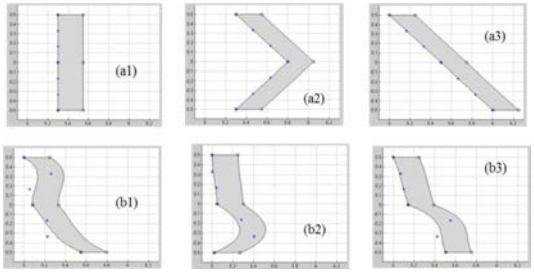

Figure 2. The parameterized Bézier curve can be used to generate planar groove structure (a1-a3) and curved groove shape structure (b1-b3).

Due to their parametric nature, Bézier curves can represent a variety of shapes by altering the coordinates of the same number of control points. In Figure 2, various Bézier curves are shown with different control points. The control points are marked with the asterisk marker whereas the resulting Bézier curve is shown with the solid line. Based on the choice of control points, these curves can generate either planar groove shape (Figure 2, a1-a3) or curved groove shape (Figure 2, b1-b3). The control points of Bézier curves are chosen as the optimization parameters to identify the optimal groove shape for micromixing. The following objective function is minimized to obtain the set of control points of Bézier curve which represents the optimal groove shape structure.

$$f(\eta) = (1-\eta)^2 \qquad (8)$$

As the maximum value η can take on is unity, the objective function is always greater than or equal to zero. The modeling-optimization algorithm is schematically shown in a flowchart in Figure 3.

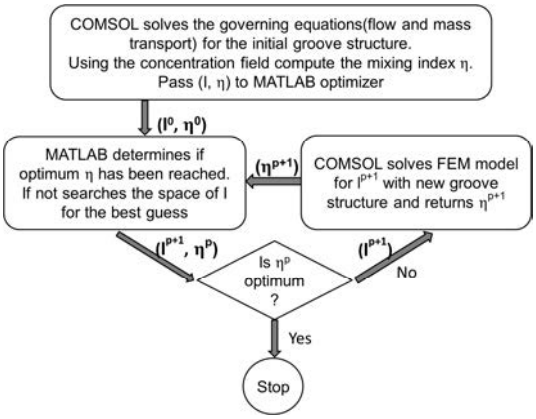

Figure 3. Flowchart Showing steps for optimization problem implementation in Comsol-Matlab.

4. Use of Comsol Multiphysics

Comsol Multiphysics 3.5a and Matlab (R2010b) are used for this computational study. The finite-element modeling part is done using Comsol Multiphysics whereas optimization is carried out using the Optimization Toolbox in Matlab. The incompressible Navier-Stokes equations and Convection-Diffusion equations from the MEMS module (Comsol Multiphysics 3.5a) are used to model the flow and species concentration distribution respectively. The mathematical model is solved with sufficiently fine mesh to ensure mesh independency of numerical results.

5. Results and Discussion

The optimization of groove structure is carried out at Q = 2 µl/min which corresponds to

the *Pe* ~ 4200. The optimal groove shape (shown in Figure 2-b2) provides the best mixing performance with η = 0.85 whereas the mixing index for conventional T-mixer is less than 0.2. Various groove types are analyzed through axial mixing index plot as shown in Figure 4. The mixing performance of the slanted groove mixer (SGM) is given by η = 0.65. The groove shape corresponding to symmetric herringbone and slanted groove are shown in Figure 2-a2 and Figure2-a3 respectively. It should be noted that the mixing performance for all groove types is identical from inlet to $\bar{x}$ = 5 as mixing in this region is due to molecular diffusion alone.

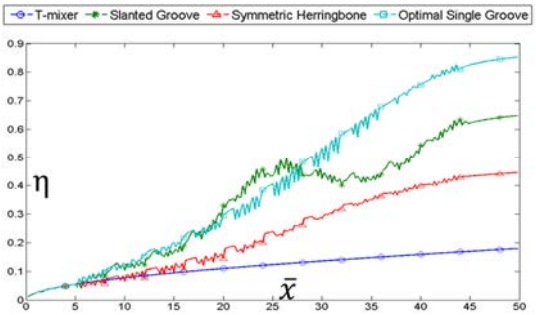

Figure 4. The axial mixing index plot for various groove designs for Pe ~ 4200.

The superior mixing performance for optimal groove structure can be understood using the cross-sectional concentration contour plots as shown in Figure 5. The optimal groove generates transverse flow to maximize the interfacial area for mass transfer as evident from Figure 5 (corresponding to $\bar{x}$ = 26 and $\bar{x}$ = 32).

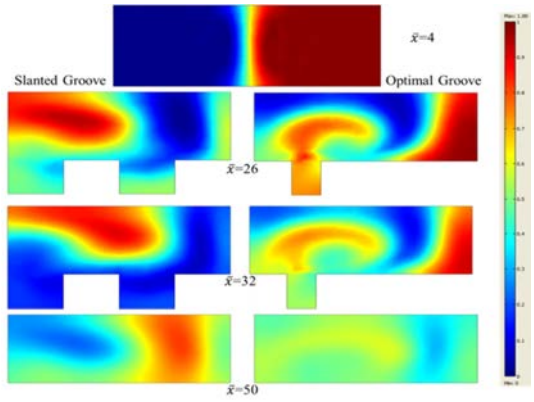

Figure 5. Cross-sectional concentration contour plots for slanted and optimal groove structure at various axial positions.

Next we evaluate the different groove types for various flow rates (Q = 0.2-3 µl/min). The optimal groove structure (identified at Q = 2 µl/min) still provides the best mixing performance for the studied range of *Pe*. The mixing performance index vs. flow rate data is shown in Figure 6 for different groove type. As the average axial flow rate is identical for all the designs, the superior mixing performance for optimal groove is solely due to generated transverse flow structure and residence time effects are not responsible for increment in mixing performance [8].

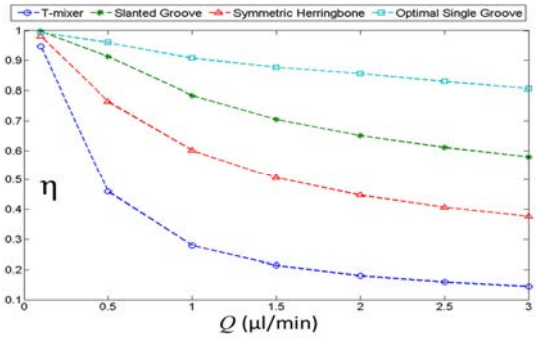

Figure 6. Variation of mixing performance with respect to the axial flow rate for different groove types.

7. Conclusions & Future Work

The effect of groove shape on the mixing performance of groove micro mixers is analyzed. The optimal groove structure is obtained by employing parametric Bézier curve representation of the groove shape. The superior mixing performance of optimal design is due to the generated transverse flow which results in higher interfacial area for mass transfer. The optimal groove is parametrically compared with other groove types and found to provide the best mixing performance for a range of *Pe* numbers studied. Currently, we are extending this study for staggered groove arrangement type and for electrokinetically driven flow based groove micromixers. The developed design optimization approach could be implemented in any microfluidic device design procedures for performance enhancement.

8. References

1. Nguyen N. T., and Wu Z. G., Micromixers - A Review, *Journal of Micromechanics and Microengineering*,**15(2)**,R1-R16 (2005).
2. Chang C. C., and Yang R. J., Electrokinetic mixing in microfluidic systems, *Microfluidics and Nanofluidics,* **3(5)**, 501-525, (2007).
3. Stroock A. D., Dertinger S. K. W., Ajdari A., Mezic I., Stone H. A., and Whitesides G. M., Chaotic Mixer for Microchannels, *Science,* **25**, 647-51, (2002).
4. Johnson T.J, Ross D, and Locascio L.E, Rapid microfluidic mixing, *Anal Chem*, **74(1)**, 45-51, (2002).
5. Kim D.S., Lee S.W, Kwon T.H and Lee S.S, A barrier embedded chaotic micromixer, *J. Micromech. Microeng*, **14**, 798-805, (2004).
6. Lynn N. S., and Dandy D. S., Geometrical optimization of helical flow in grooved micromixers, *Lab on a Chip*, **7**,580-587, (2007).
7. Jain M., Yeung A., and Nandakumar K., Induced charge electro osmotic mixer: Obstacle shape optimization, *Biomicrofluidics*, **3**,022413 (2009).
8. Jain M, and Nandakumar K., Novel index for micromixing characterization and comparative analysis, *Biomicrofluidics,* **4(3)**:031101 (2010).

9. Acknowledgements

Authors would like to acknowledge the use of computing facilities of the Louisiana Optical Network Initiative (LONI) & High Performance Computing (HPC) facility at Louisiana State University and the continued funding from the Cain Chair program.

10. Appendix

Table 1: Geometric Parameters

Parameter	Value	Description
W $(\bar{W})$	200 μm 1	Width of the microchannel (Along y-axis (from $\bar{y} = 0.5\ to -$ 0.5)
L $(\bar{L})$	1 cm 50	Length of microchannel (Along x-axis) (from $\bar{x} = 0\ to\ 50$)
H $(\bar{H})$	80 μm 0.4	Height of microchannel (Along z-axis) (from $\bar{z} = 0\ to$ 0.4)
a	50 μm	Groove width
b	50 μm	Groove spacing
p	250 μm	Groove cycle spacing
H_G	40 μm	Groove height (from $\bar{z} = 0\ to -$ 0.2)